Preprints of the 18th IFAC World Congress
Milano (Italy) August 28 - September 2, 2011

Maximisation of Energy Capture by a Wave-Energy Point Absorber using Model Predictive Control

J. A. M. Cretel*. G. Lightbody.**
G. P. Thomas*. A. W. Lewis*.**

**Hydraulics & Maritime Research Centre, University College Cork, Cork, Ireland (Tel: (+353)(0)21 4250031; e-mail: j.cretel@umail.ucc.ie).*
***Department of Electrical and Electronic Engineering, University College Cork, Cork, Ireland.*
****School of Mathematical Sciences, University College Cork, Cork, Ireland.*

Abstract: Wave-energy point absorbers can be defined as oscillators excited by ocean waves. Devices of this kind are meant to be deployed offshore for the production of renewable energy. As wave conditions at a given site can vary widely over time, advanced control strategies for point absorbers are required to guarantee good performance. This article presents a state-space control scheme for a point absorber, which builds on an approach outlined in an earlier article by the same authors. Strongly based on model predictive control (MPC), the control scheme makes use of an unusual form of the objective function, and aims at maximising the production of energy by the point absorber. The control scheme remedies some of the shortcomings of existing approaches to the control of a point absorber, such as *reactive control* and *latching control*, and is meant to be extendable to any point absorber that can be well described by a linear model. Results of numerical simulations of a heaving point absorber controlled with this scheme are presented and confirm the potential of this approach.

Keywords: wave energy, point absorber, model predictive control, reactive control, latching control, convex optimization, quadratic programming.

1. INTRODUCTION

1.1 Control of wave-energy point absorbers

Wave-energy capture is a much anticipated technology meant to produce renewable energy from ocean waves. Point absorbers (Falnes, 2002a) arguably figure among the most promising wave-energy concepts proposed so far. Point absorbers come in a variety of forms, but can generally be described as relatively small, linear, damped oscillators excited by ocean waves. Incident waves put the mass element of the system—which may consist of a floating or submerged body, or a water column oscillating within a plenum—into motion, motion which is resisted by some power take-off (PTO) machinery; useful energy can therefore be produced and transmitted to shore. Point absorbers are expected to be deployed offshore at the commercial stage, in arrays of several units known as *wave farms*. Control strategies that improve the capacity of point absorbers to extract energy from the waves are desirable, as passive control (using a fixed linear damping) typically yields poor performance. A point absorber must be able to adapt its behaviour to the wave climate, which may vary dramatically at a given site. Control of wave-energy converters has been the subject of numerous research articles since the 1970s; the reader may refer to Falnes (2002b) and Salter, Taylor and Caldwell (2002) for an overview of the field. Two of the most studied approaches to control of point absorbers are briefly reviewed here.

Reactive control (Budal & Falnes, 1977) is, historically, the first approach to controlling point absorbers and is primarily based on hydrodynamic considerations. It stems from frequency-domain modelling of point-absorber dynamics and amounts to setting the value of the (mechanical) load so as to maximise absorption of mechanical energy by the system. It is the mechanical analogue to what is known as *impedance matching* in the context of linear electrical circuits. For this reason, and because the term *reactive control* can be misleading, the term *impedance matching* (or *mechanical impedance matching*, to avoid a dispute in terminology) should perhaps be preferred. Impedance matching can be articulated in the time domain (Naito & Nakamura, 1985), though information on the future wave excitation is required to apply it. Although it is meant to yield maximum energy absorption by the point absorber, impedance matching suffers from both theoretical and practical limitations. A theoretical limitation is that it may prescribe unrealistically large oscillations, and a practical limitation is that it may require prohibitively large amounts of energy flowing up and down the energy conversion chain.

An alternative to impedance matching that has become known as *latching control* was proposed by Falnes & Budal (1978). Latching consists of an alternation of phases during which the oscillator is linearly damped by the PTO and phases during which it is locked into position (i.e. *latched*) by a mechanism of some description. Latching control, therefore, contrary to impedance matching, requires no reversal of the energy flowing between the sea and the system. As with impedance matching, latching control also requires information on the future wave excitation. If the point absorber is latched and released in a timely fashion, an artificial resonance can be achieved, thereby greatly improving performance over merely using a fixed, linear damping. Originally developed for the case of sinusoidal wave excitation, latching control was extended to irregular waves by Hoskin (1988), who made use of Pontryagin's Maximum Principle. The same technique was later applied by Babarit & Clément (2006), who used a state-space model for describing the wave radiation phenomenon. Eidsmoen (1998) modified the basic principle of latching with the intent of handling amplitude constraints. Falcão (2007) proposed an alternative on-off control strategy, which requires no knowledge of the future wave excitation, with a view to applying it to point absorbers equipped with a hydraulic PTO. Despite its widespread popularity in the wave-energy literature, however, the latching approach has some key limitations. In particular, its suitability to point absorbers equipped with electrical PTO has not been assessed; moreover, latching control may prove inadequate for arrays of point absorbers, since the optimum phase condition on which it is founded does not hold if more than one oscillator are present (Falnes, 1980; Thomas & Evans, 1981).

New control approaches are required. The development of better PTO systems for point absorbers, such as linear electrical generators and novel variable-displacement hydraulics (Payne *et al.*, 2005), has opened the possibility of devising control strategies that would optimise the control force in real time, as advocated by Salter, Taylor & Caldwell (2002) and Molinas *et al.* (2007). Model predictive control (MPC) is an advanced control methodology (Maciejowski, 2002; Rossiter, 2003) that lends itself well to that kind of approach.

1.2 MPC applied to point absorbers

The first foray in that direction was made by Gieske (2007). His numerical study focused on a point-absorber concept known as the Archimedes Wave Swing, of which a linearised model was used. Although Gieske modelled the action of wave radiation on the system rather simplistically, using a linear damper, he can be credited for proposing a number of novel ideas that would later be revisited by other wave-energy researchers (Cretel *et al.*, 2010; Fusco & Ringwood, 2010; Hals, Falnes & Moan, 2011):

- associating the objective function with the amount of energy produced by the point absorber over the prediction horizon;
- estimating the wave-excitation force from the motion of the device (with the proviso that a sufficiently accurate model of the system be used in the control algorithm);
- predicting the wave-excitation force over the horizon by fitting a linear static auto-regressive model to the sequence of excitation-force estimates and propagating that model forward in time.

A later article by Hals, Falnes & Moan (2011) is of importance here. In that theoretical study, MPC was applied to a heaving, semi-submerged sphere constrained to oscillate over a finite stroke. The model developed by Hals stems from linearised wave-structure interactions and includes a low-order linear state-space model dedicated to the wave-radiation phenomenon; the PTO system is assumed ideal. Most peculiarly, the formulation of the objective function involves two different state-space systems; this is hardly necessary, though, as shown in the present paper. Besides, Hals uses the vector of predicted velocities as the optimisation variable, a questionable choice because the power-take-off force, not the oscillator's velocity, is the controllable input to the system; optimising the trajectory with respect to the vector of predicted inputs, as in the present article, is more general. Hals considers two objective functions for his MPC algorithm: one corresponds to the difference between the energy entering the system and the energy radiated away from the system over the prediction horizon; the other corresponds to the power absorbed by the PTO system over the prediction horizon. Hals deems the first objective function preferable to the second one, which is reported to yield "inaccurate solutions". It should be noted, however, that those two objective functions correspond to different optimisation problems: the second objective function penalizes the energy stored in the system, in potential and kinetic form, at the end of the prediction horizon, whereas the first one does not. The solutions to those two optimisation problems may, therefore, be different. Hals also reports unwanted, fast fluctuations in the "optimal" PTO force, which he suggests could be subsequently low-pass filtered, in practice. However, these numerical difficulties can simply be circumvented by the addition of *regularization terms* (Boyd & Vandenberghe, 2004) in the objective function. In Hals, Falnes & Moan (2011), information on the future wave-excitation force is obtained via a method reminiscent of that used by Budal *et al.* (1982). A nonlinear, time-varying system is used to model the wave-excitation process. State estimates of this system are derived by feeding measurements of the wave-excitation force to an extended Kalman filter, which is then used to obtain a multistep prediction of the wave excitation. Hals reports disappointing results in terms of prediction accuracy, using that technique, but other, arguably better, methods of time-series prediction can be used (Fusco & Ringwood, 2010).

Bacelli, Gilloteaux & Ringwood (2009) also deserve mention, on account of the combination of MPC and dynamic programming (Bertsekas, 2005) they proposed for the control of a nonlinear point-absorber system dedicated to potable-water production.

Of particular interest here, however, is an earlier paper by Cretel *et al.* (2010), which introduced an MPC-based control methodology meant to maximise the energy capture by a point absorber. The approach put forth in that preliminary article allowed for the estimation, by soft sensing, and the short-term prediction of the wave-excitation force, prediction which could be used in the predictive control algorithm. The present article improves the methodology outlined in Cretel *et al.* (2010). The use of a triangle hold for the model inputs and a refinement of the objective function yield better results than those reported earlier. Moreover, the addition of penalty terms in the objective function alleviates the need for an excessive flow of mechanical reactive power associated with the control action, a problem which was noted by both Cretel *et al.* (2010) and Hals, Falnes & Moan (2011). The new control formulation is tested numerically on a heaving point absorber of cylindrical shape, excited by regular or irregular waves, and either free or subject to amplitude constraints.

2. MATHEMATICAL MODEL

2.1 Equation of motion

Consider a floating body of structural mass m and constrained to oscillate in heave (i.e. in the vertical direction) only. Let z denote the vertical displacement of the float with respect to its position at rest (see figure 1).

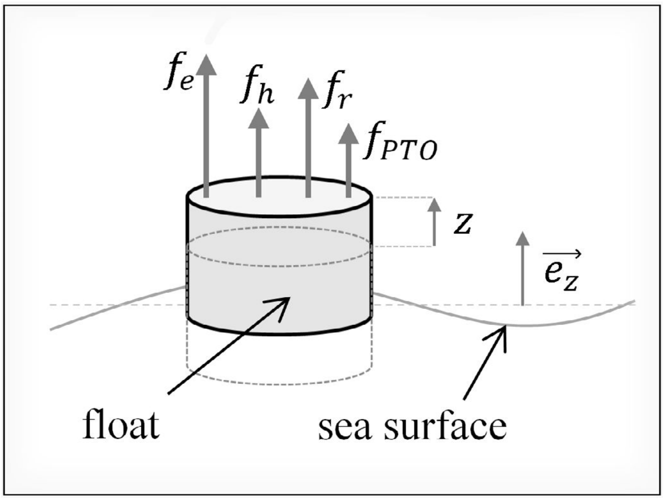

Fig. 1. Schematic view of the floating body and the forces exerted on it; the dotted cylinder corresponds to the float at rest, and the dotted line to the sea surface in calm water (no waves).

Assume the chosen frame of reference to be inertial; the time-domain equation of motion, according to Newton's second law of motion, is

$$m\ddot{z}(t) = f_h(t) + f_e(t) + f_r(t) + f_{PTO}(t), \quad (1)$$

where t denotes time and f_{PTO} the force exerted by the PTO system on the floating body. The other three forces, f_h, f_e and f_r follow from linear wave theory (Newman, 1977), which is assumed throughout the article:

- the hydrostatic restoring force f_h, expressed in terms of the hydrostatic stiffness k_h and z, reflects the spring-like effect of the fluid surrounding the body:

$$f_h(t) = -k_h z(t); \quad (2)$$

- the wave-excitation force f_e reflects the interactions between incident waves and the body held fixed at its equilibrium position;
- the radiation force f_r is associated with the waves radiated by the body oscillating in calm water.

The radiation force accounts for two distinct effects that the water has on the floating body: it *i)* modifies the apparent inertia of the float and *ii)* damps the motion of the float. The radiation force is usually expressed, according to Cummins (1962), as

$$f_r(t) = -\mu\ddot{z}(t) - \int_{-\infty}^{t} h_r(\tau)\dot{z}(t-\tau)d\tau, \quad (3)$$

where μ is the so-called *added mass at infinity* and h_r is the so-called *retardation function*. The quantities k_h and μ and the function h_r can all be computed with codes dedicated to the analysis of wave interactions with floating bodies, such as WAMIT®, which was used for this study.

Introducing the forces per unit mass

$$u_c(t) = \frac{f_{PTO}(t)}{m+\mu}, \quad (4)$$

$$v_c(t) = \frac{f_e(t)}{m+\mu}, \quad (5)$$

and combining (1-5) yields a new expression for the equation of motion:

$$\ddot{z}(t) + \frac{1}{m+\mu}\int_{-\infty}^{t} h_r(\tau)\dot{z}(t-\tau)d\tau + \frac{k_h}{m+\mu}z(t) = u_c(t) + v_c(t). \quad (6)$$

This differential equation describes a non-autonomous, linear time-invariant (LTI) system with two inputs: the control input u and an uncontrollable input v which corresponds to the wave excitation. A state-space model of this continuous-time system is derived in the next subsection.

2.2 State-space representation of the system

Equation 6, being of an integro-differential form, must be modified before a state-space model of the point absorber can be derived. In particular, the integral term in (6) must be approximated. It corresponds to the output of a (causal) LTI system of impulse-response function (IRF) h_r and which takes the velocity $\dot{z}$ as input; for convenience, this system will subsequently be referred to as the *radiation subsystem* in the present article. The function h_r is related to the frequency-dependent added mass and radiation damping (Falnes, 2002a) and may be obtained from codes such as WAMIT®. These codes, however, cannot produce an analytical expression for h_r, only sampled data of it; the radiation subsystem must therefore be identified on the basis of those sampled data. One identification technique applicable in that case is Prony's method, which is meant to produce a rational transfer function closely fitting samples of the impulse response. The rational function may be either discrete-time, as in Hayes (1996), or continuous-time, as in Duclos, Clément & Chatry (2001). By applying Prony's method to the sampled data of h_r obtained via WAMIT®, an n^{th}-order, continuous-time, rational transfer-function model of the radiation subsystem is obtained:

$$\widehat{H}_r(s) = \frac{b_1 s^{n-1} + \cdots + b_n}{s^n + a_1 s^{n-1} + \cdots + a_n}, \quad (7)$$

where $\widehat{H}_r(s)$ is the Laplace transform of the approximation $\hat{h}_r(t)$ based on the sequence of samples $\{h_r(k)\}_k$. A state-space realization of this system is then adopted:

$$\dot{\boldsymbol{x}}_{\boldsymbol{r}}(t) = A_r \boldsymbol{x}_{\boldsymbol{r}}(t) + B_r \dot{z}(t),$$
$$\int_{-\infty}^{t} h_r(\tau)\dot{z}(t-\tau)d\tau \approx C_r \boldsymbol{x}_{\boldsymbol{r}}(t),$$

where $\boldsymbol{x}_{\boldsymbol{r}} \in \mathbb{R}^n$, $A_r \in \mathbb{R}^{n\times n}$, $B_r \in \mathbb{R}^{n\times 1}$ and $C_r \in \mathbb{R}^{1\times n}$. For this preliminary study, the (top-companion) control canonical form was chosen for the state-space realization. The order of the transfer-function model (7) should in practice be chosen large enough to obtain a good approximation of h_r, but small enough not to compromise the real-time tractability of the control algorithm that is developed in the following.

The state vector $\boldsymbol{x}_{\boldsymbol{c}}$ and output vector $\boldsymbol{y}_{\boldsymbol{c}}$ of the continuous-time model representing the whole point-absorber system are defined as

$$\boldsymbol{x}_{\boldsymbol{c}} = \begin{bmatrix} z \\ \dot{z} \\ \boldsymbol{x}_{\boldsymbol{r}} \end{bmatrix} \in \mathbb{R}^{n+2},$$
$$\boldsymbol{y}_{\boldsymbol{c}} = \begin{bmatrix} z \\ \dot{z} \end{bmatrix} \in \mathbb{R}^2.$$

The state vector $\boldsymbol{x}_{\boldsymbol{r}}$ of the radiation subsystem has been included in the state vector $\boldsymbol{x}_{\boldsymbol{c}}$ of the whole system, as it contains information on the state of the surrounding fluid. Both z and $\dot{z}$ are assumed to be measured, hence their inclusion in the output vector $\boldsymbol{y}_{\boldsymbol{c}}$. The associated dynamics and output equations are:

$$\dot{\boldsymbol{x}}_{\boldsymbol{c}}(t) = A_c \boldsymbol{x}_{\boldsymbol{c}}(t) + B_c\big(u_c(t) + v_c(t)\big),$$
$$\boldsymbol{y}_{\boldsymbol{c}}(t) = C_c \boldsymbol{x}_{\boldsymbol{c}}(t),$$

where

$$A_c = \begin{bmatrix} 0 & 1 & \mathbf{0} \\ \frac{-k_h}{(m+\mu)} & 0 & \frac{-1}{(m+\mu)}C_r \\ \mathbf{0} & B_r & A_r \end{bmatrix} \in \mathbb{R}^{(n+2)\times(n+2)},$$
$$B_c = \begin{bmatrix} 0 \\ 1 \\ \mathbf{0} \end{bmatrix} \in \mathbb{R}^{(n+2)\times 1},$$
$$C_c = \begin{bmatrix} 1 & 0 & \mathbf{0} \\ 0 & 1 & \mathbf{0} \end{bmatrix} \in \mathbb{R}^{2\times(n+2)}.$$

The symbol $\mathbf{0}$ denotes a zero matrix of required dimensions. This system is assumed stable and the dynamics matrix, A_c, is assumed non-singular. A discretised version of this continuous-time system is now required for use in the control algorithm.

2.3 Discretisation of the continuous-time system

Introduce the update interval $h > 0$ and let $\boldsymbol{x}_{\boldsymbol{d}}$, $\boldsymbol{y}_{\boldsymbol{d}}$, u_d and v_d denote the sampled versions of $\boldsymbol{x}_{\boldsymbol{c}}$, $\boldsymbol{y}_{\boldsymbol{c}}$, u_c and v_c. The state transition from time kh to time $(k+1)h$ is given by

$$\boldsymbol{x}_{\boldsymbol{d}}(k+1) = \phi(h)\boldsymbol{x}_{\boldsymbol{d}}(k) + \int_{kh}^{kh+h} \phi(kh+h-\tau)B_c\big(u_c(\tau)+v_c(\tau)\big)d\tau, \quad (8)$$

where $\forall\, t,\ \phi(t) \triangleq e^{tA_c}$. In an earlier article (Cretel *et al.*, 2010), a zero-order hold was used for the inter-sample behaviour of the inputs. A triangle hold (Franklin, Powell & Workman, 1990), whereby the inputs u and v are continuous piecewise linear, is preferred here, for two reasons: *i)* it reduces the need for a short update interval h, thus decreasing the complexity of the optimization problem associated with the control algorithm, without compromising the length of the prediction horizon; *ii)* it is convenient for deriving an expression of the product $u_d(k)\dot{z}(k)$, which plays a key role in the formulation of the objective function. Only an approximation of this product was used in Cretel *et al.* (2010), whereas the exact expression is used here. Using a triangle hold for both inputs u_c and v_c means that

$$\forall\, k \in \mathbb{N},\quad \forall\, t \in [kh, (k+1)h],$$
$$u_c(t) = u_d(k) + \tfrac{t-kh}{h}\Delta u(k+1), \quad (9)$$
$$v_c(t) = v_d(k) + \tfrac{t-kh}{h}\Delta v(k+1), \quad (10)$$

where $\Delta u(k+1) \triangleq u_d(k+1) - u_d(k)$,
$\Delta v(k+1) \triangleq v_d(k+1) - v_d(k)$.

After substitution of (9-10) in (8), the following triangle-hold equivalent of the continuous-time system is obtained:

$$\boldsymbol{x}_{\boldsymbol{d}}(k+1) = \phi(h)\boldsymbol{x}_{\boldsymbol{d}}(k) + \Gamma\big(u_d(k)+v_d(k)\big) + \Lambda\big(\Delta u(k+1) + \Delta v(k+1)\big), \quad (11)$$
$$\boldsymbol{y}_{\boldsymbol{d}}(k) = C_c \boldsymbol{x}_{\boldsymbol{d}}(k), \quad (12)$$

where $\Gamma \triangleq {A_c}^{-1}(\phi(h) - I)B_c \in \mathbb{R}^{(n+2)\times 1}$,
$\Lambda \triangleq \frac{1}{h}{A_c}^{-1}(\Gamma - hB_c) \in \mathbb{R}^{(n+2)\times 1}$.

2.4 State and output augmentation

The state vector of system (11-12) is then augmented by the two inputs, u_d and v_d, while the output vector is augmented by u_d only; this augmentation facilitates the formulation of the objective function that is used in the proposed control scheme. The input increments Δu and Δv thus play the role of inputs to the new system (13-14). Define the augmented state vector $\boldsymbol{x}$ and output vector $\boldsymbol{y}$ as

$$\boldsymbol{x} = \begin{bmatrix} \boldsymbol{x}_{\boldsymbol{d}} \\ u_d \\ v_d \end{bmatrix} \in \mathbb{R}^{n+4},$$
$$\boldsymbol{y} = \begin{bmatrix} \boldsymbol{y}_{\boldsymbol{d}} \\ u_d \end{bmatrix} \in \mathbb{R}^3.$$

The associated state-space equations are

$$\boldsymbol{x}(k+1) = A\boldsymbol{x}(k) + B\Delta u(k+1) + F\Delta v(k+1), \quad (13)$$
$$\boldsymbol{y}(k) = C\boldsymbol{x}(k), \quad (14)$$

where

$$A = \begin{bmatrix} \phi(h) & \Gamma & \Gamma \\ 0 & 1 & 0 \\ 0 & 0 & 1 \end{bmatrix} \in \mathbb{R}^{(n+4)\times(n+4)},$$
$$B = \begin{bmatrix} \Lambda \\ 1 \\ 0 \end{bmatrix} \in \mathbb{R}^{(n+4)\times 1},$$
$$F = \begin{bmatrix} \Lambda \\ 0 \\ 1 \end{bmatrix} \in \mathbb{R}^{(n+4)\times 1},$$

$$C = \begin{bmatrix} 1 & 0 & 0 & \cdots & 0 & 0 & 0 \\ 0 & 1 & 0 & \cdots & 0 & 0 & 0 \\ 0 & 0 & 0 & \cdots & 0 & 1 & 0 \end{bmatrix} \in \mathbb{R}^{3\times(n+4)}.$$

3. CONTROL FORMULATION

3.1 Observability and controllability

The system is assumed observable. The state vector, $\boldsymbol{x}(k)$, is assumed known here, but future work will focus on including a state estimator in the control scheme. An interesting consequence of the observability of system (13-14) is that the wave-excitation force per unit mass, v_d, can be estimated by soft sensing. Moreover, a sequence of v_d estimates could serve as a basis for predicting v_d in the short term; this prediction could then be used in the control algorithm. The controllability matrix has a rank deficiency of (at least) 1, as can be expected from the way matrices A and B are constructed: input Δu does not affect state variable v_d.

3.2 MPC formulation

Let N denote the length of the prediction horizon and introduce the prediction vector notation

$$\underline{\boldsymbol{\xi}}(k) = \begin{bmatrix} \boldsymbol{\xi}(k+1|k) \\ \vdots \\ \boldsymbol{\xi}(k+N|k) \end{bmatrix}$$

to represent the prediction of a (vector or scalar) variable $\boldsymbol{\xi}$ over the prediction horizon, based on information available at time k.

The output prediction vector, $\underline{\boldsymbol{y}}(k)$, can therefore be written as a function of the current state and the future input increments:

$$\underline{\boldsymbol{y}}(k) = \mathcal{P}\boldsymbol{x}(k) + \mathcal{T}_u\underline{\Delta\boldsymbol{u}}(k) + \mathcal{T}_v\underline{\Delta\boldsymbol{v}}(k), \tag{15}$$

where $\mathcal{P} = \begin{bmatrix} CA \\ CA^2 \\ \vdots \\ CA^N \end{bmatrix} \in \mathbb{R}^{3N\times(n+4)}$,

and where $\mathcal{T}_u$ and $\mathcal{T}_v$ are block Toeplitz matrices (refer to Maciejowski, 2002, or Rossiter, 2003):

$$\mathcal{T}_u = \begin{bmatrix} CB & 0 & 0 & \cdots \\ CAB & CB & 0 & \cdots \\ CA^2B & CAB & CB & \cdots \\ \vdots & \vdots & \vdots & \vdots \\ CA^{N-1}B & CA^{N-2}B & CA^{N-3}B & \cdots \end{bmatrix} \in \mathbb{R}^{3N\times N},$$

$$\mathcal{T}_v = \begin{bmatrix} CF & 0 & 0 & \cdots \\ CAF & CF & 0 & \cdots \\ CA^2F & CAF & CF & \cdots \\ \vdots & \vdots & \vdots & \vdots \\ CA^{N-1}F & CA^{N-2}F & CA^{N-3}F & \cdots \end{bmatrix} \in \mathbb{R}^{3N\times N}.$$

3.3 Objective function

In this preliminary study, the control objective is simply to maximise the energy produced by the point-absorber system over the prediction horizon, at each time step; the PTO machinery is assumed ideal, which implies that the absorbed mechanical energy coincides with the useful energy. Furthermore, the wave excitation over the horizon is assumed to be provided to the control algorithm; i.e., at any time k, vector $\underline{\Delta\boldsymbol{v}}(k)$ is assumed known. The quantity to be maximised can be written as

$$E_{t,t+T} \triangleq -(m+\mu)\int_t^{t+T} u(\tau)\dot{z}(\tau)d\tau.$$

where T is the length of the time horizon. By applying the trapezoidal rule of numerical integration with subinterval h, an approximation of this integral is obtained:

$$E_{t,t+T} \approx -(m+\mu)h\left(\tfrac{1}{2}u_d(k)\dot{z}(k) + \sum_{i=k+1}^{k+N-1} u_d(i|k)\dot{z}(i|k) + \tfrac{1}{2}u_d(k+N|k)\dot{z}(k+N|k)\right). \tag{16}$$

Objective function J_1 is then derived from (16), as

$$J_1(k) \triangleq \sum_{i=k+1}^{k+N-1} u_d(i|k)\dot{z}(i|k) + \tfrac{1}{2}\, u_d(k+N|k)\dot{z}(k+N|k). \tag{17}$$

Note that this objective function must be minimised, since the negative multiplying factor $-(m+\mu)h$ from the discrete approximation (16) has been omitted in the expression of J_1. Furthermore, $J_1(k)$ is to be minimised at time k, after $u_d(k)$ has been applied; the term $1/2\ u_d(k)\dot{z}(k)$, which appears in (16), has therefore been discarded in the expression of the objective function (17). Note that the form of cost $J_1(k)$ departs from that of "conventional" MPC, in which a set-point trajectory is provided and the associated optimisation problem is a discrete least-squares problem. No set-point trajectory is available here; the trajectory yielding maximum absorption of energy is not known in advance and the objective function cannot, therefore, be expressed as the square of the 2-norm of a predicted tracking error. Nevertheless, it can be formulated as a quadratic function of the optimization variable $\underline{\Delta\boldsymbol{u}}$. Consider first that the cost can be written in terms of the output prediction vector $\underline{\boldsymbol{y}}(k)$:

$$J_1(k) = \tfrac{1}{2}\underline{\boldsymbol{y}}^T(k)Q\underline{\boldsymbol{y}}(k), \tag{18}$$

where $Q \in \mathbb{R}^{3N\times 3N}$ is a block diagonal matrix defined as

$$Q \triangleq \begin{bmatrix} M & & & \\ & \ddots & & \\ & & M & \\ & & & \tfrac{1}{2}M \end{bmatrix},$$

and $$M \triangleq \begin{bmatrix} 0 & 0 & 0 \\ 0 & 0 & 1 \\ 0 & 1 & 0 \end{bmatrix}.$$

Substituting (15) in (18) then yields

$$J_1 = \frac{1}{2}\underline{\Delta\boldsymbol{u}}^T\mathcal{T}_u{}^TQ\mathcal{T}_u\underline{\Delta\boldsymbol{u}} + \underline{\Delta\boldsymbol{u}}^T\mathcal{T}_u{}^TQ\left(\mathcal{P}\boldsymbol{x} + \mathcal{T}_v\underline{\Delta\boldsymbol{v}}\right) + \tfrac{1}{2}\left(\mathcal{P}\boldsymbol{x} + \mathcal{T}_v\underline{\Delta\boldsymbol{v}}\right)^TQ\left(\mathcal{P}\boldsymbol{x} + \mathcal{T}_v\underline{\Delta\boldsymbol{v}}\right), \tag{19}$$

where time dependence has been omitted for lighter appearance. The Hessian of this objective function, $\mathcal{T}_u{}^T Q \mathcal{T}_u$, is assumed positive semi-definite; minimising $J_1(k)$ therefore amounts to solving a convex quadratic programming (QP) problem (Boyd & Vandenberghe, 2004). Constraints on the oscillation amplitude or velocity (or both) of the point absorber may be specified by affine inequality constraints on $\underline{\Delta \boldsymbol{u}}$. Hard constraints on the PTO force can also be specified by affine inequality constraints on $\underline{\Delta \boldsymbol{u}}$ but may give rise to feasibility issues; no such constraints are considered herein. The corresponding constrained QP problem,

$$\text{minimise } J_1(k)$$
$$\text{so that } \underline{\Delta \boldsymbol{u}}(k) \in D$$

where D is the feasible set defined by the constraints, is therefore also convex. The last term in (19) does not depend on the optimization variable $\underline{\Delta \boldsymbol{u}}$ and can be discarded, which leads to the definition of a new objective function:

$$J_2 \triangleq \frac{1}{2} \underline{\Delta \boldsymbol{u}}^T \mathcal{T}_u{}^T Q \mathcal{T}_u \underline{\Delta \boldsymbol{u}} + \underline{\Delta \boldsymbol{u}}^T \mathcal{T}_u{}^T Q \left(\mathcal{P} \boldsymbol{x} + \mathcal{T}_v \underline{\Delta \boldsymbol{v}} \right).$$

Furthermore, a penalty term quadratic in $\underline{\Delta \boldsymbol{u}}$ is introduced here in order to limit the aggressiveness of the control:

$$J_3(k) \triangleq J_2(k) + \lambda \left\| \underline{\Delta \boldsymbol{u}}(k) \right\|_2^2, \qquad (20)$$

where λ is a non-negative weight which has the dimension of a time. As J_1 is a convex function of $\underline{\Delta u}$, J_3 is also convex.

It may be desirable to add other terms to objective function J_3 in order to reduce the reactive power—be it electrical, mechanical or otherwise—associated with the control. As will be shown in the next section (see figure 6), the control may give rise to large amounts of energy flowing in and out of the system. The time-average of the power produced by the point absorber may be positive, but the instantaneous power may undergo large excursions in both the positive direction and the negative direction. This large, reversing flow of energy is no cause for concern in theory, when the PTO system is assumed ideal, but it may be problematic in practice: some PTO systems are not able to work in all four quadrants, all real PTO systems have a limited power rating, and some resistive losses arise during their operation. Penalty terms reflecting those resistive losses can be added to the cost so as to obtain a better control, with the proviso that the addition of these terms not compromise the convexity of the objective function. To demonstrate this possibility, and although only an ideal PTO system has been considered herein, a penalty term quadratic in $\underline{\boldsymbol{u}}$ is added to the cost J_3:

$$J_4(k) \triangleq J_3(k) + \lambda' \left\| \underline{\boldsymbol{u}}(k) \right\|_2^2,$$

where λ' is a non-negative weight which, like λ, has the dimension of a time. Since

$$\underline{\boldsymbol{u}}(k) = L \underline{\Delta \boldsymbol{u}}(k) + u_d(k) \mathbf{1},$$

where $L \in \boldsymbol{R}^{N \times N}$ is a lower triangular matrix filled with 1's and $\mathbf{1}$ is an N-vector filled with 1's, it can be shown that $\left\| \underline{\boldsymbol{u}}(k) \right\|_2^2$ is a convex function of $\underline{\Delta \boldsymbol{u}}(k)$; therefore, so is $J_4(k)$. As in conventional MPC, the control algorithm consists in applying, at every time k, the first component of

$$\underline{\Delta \boldsymbol{u}}^*(k) \triangleq \underset{\underline{\Delta \boldsymbol{u}}(k) \in D}{\operatorname{argmin}} \left(J_4(k) \right)$$

which is obtained with some QP solver.

4. SIMULATION RESULTS

Numerical simulations were run for a semi-immersed float of cylindrical shape, of radius 5 m and draft 8 m, in deep water (Newman, 1977). A sampling time of 0.1 s was used. A fifth-order model for the radiation subsystem was used, as it was found to give a good compromise between approximation accuracy and size of the model (see figure 2). The initial condition for x was chosen as $\mathbf{0}$ for all simulations.

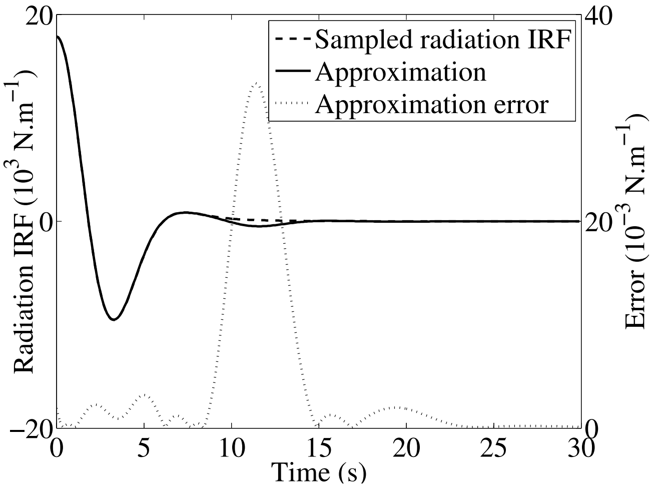

Fig. 2. Approximation of the radiation subsystem by a 5$^{\text{th}}$-order transfer-function model.

Cost J_4 was used in the control algorithm. Unless otherwise stated, the horizon length was set to $N = 60$ and weight λ' was set to 0 s; weight λ set to 2 s for all simulations.

Figure 3 shows that the results are in accordance with those obtained by applying *mechanical impedance matching* (i.e. reactive control): the velocity and the wave-excitation force are approximately in phase (refer to Falnes, 2002a).

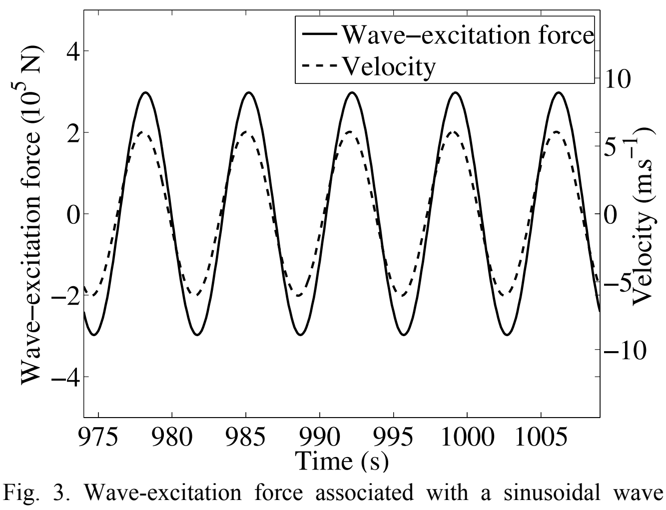

Fig. 3. Wave-excitation force associated with a sinusoidal wave (amplitude: 1 m; period: 7 s) and velocity of the unconstrained point absorber.

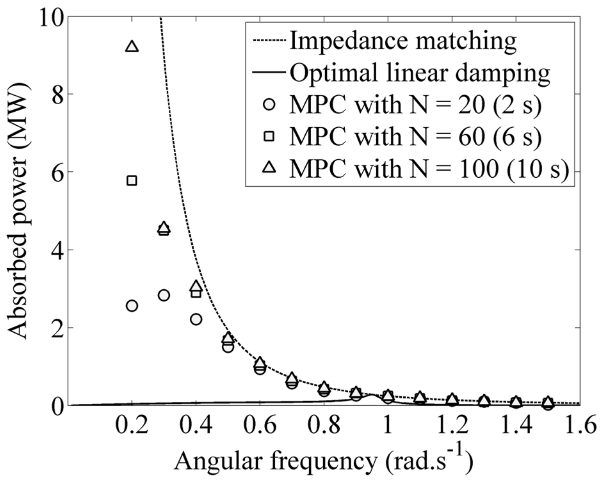

Fig. 4. Mean rate of energy absorbed by an unconstrained point absorber against angular frequency of sinusoidal wave excitation. The data points were obtained by running the control algorithm for different wave-excitation frequencies and horizon length; the post-transient mean absorbed power was computed for each case. Power curves corresponding to mechanical impedance matching and optimal linear damping have been included for comparison.

Figure 4 seems to corroborate the proposition that longer prediction horizons yield better performance. It appears to be the case here, in the low-frequency range in particular, which is in accordance with intuition. This observation should be treated with caution, though: Bertsekas (2005) provides a generic counterexample in which a longer horizon actually leads to poorer performance. It is unclear, at this stage, how the length of the prediction horizon ought to be set, but figure 4 indicates that using a time horizon as long as the "time span" of the impulse-response function may be well-advised. In this connection, a theoretical study by Price, Forehand & Wallace (2009), which investigates how far into the future the wave excitation should ideally be predicted, may be of interest to the reader.

The simulations reported by figures 5-7 were 1024 s long, and involved a point absorber excited by irregular waves (Bretschneider spectrum; significant wave height: 3 m; zero-upcrossing period: 8 s), whose float was constrained to oscillate in heave between -5 m and +5 m.

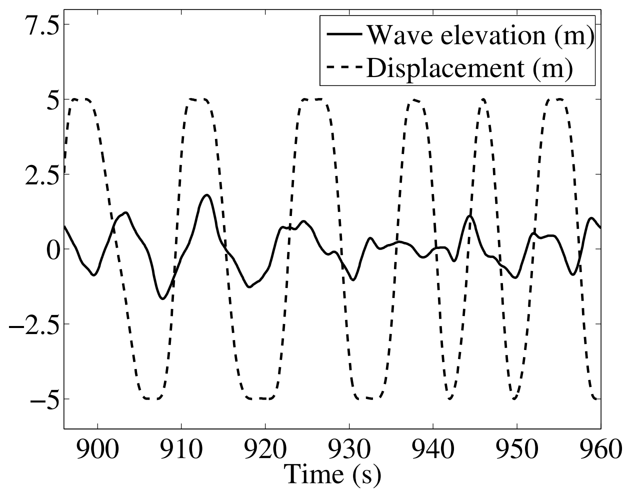

Fig. 5. Irregular wave elevation and displacement of the constrained point absorber.

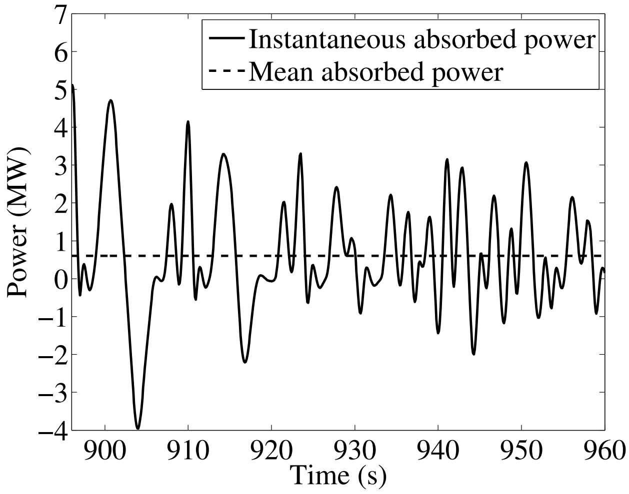

Fig. 6. Power signal obtained for the constrained point absorber excited by irregular waves ($\lambda' = 0\ s$).

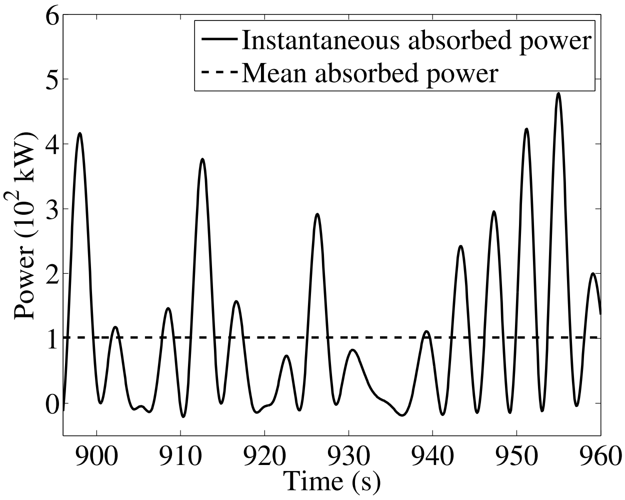

Fig. 7. Power signal obtained for the constrained point absorber excited by irregular waves ($\lambda' = 2$ s).

Figure 5 indicates that the control algorithm is effective in keeping the system within the specified amplitude constraints. Figure 6 illustrates the reactive-power problem mentioned at the end of the preceding section, and figure 7 shows how setting λ' to some positive value (2 s, here) solves that problem by compelling the point absorber to almost strictly absorb energy, without returning any to the sea.

5. CONCLUSION

A control scheme based on MPC and meant to maximise the energy capture of a wave-energy point absorber has been presented. The departure from conventional MPC is twofold:

- A triangle hold, instead of the usual zero-order hold, is used for discretising the continuous-time system;
- A non-standard form of objective function is adopted, that does not involve any set-point trajectory.

The control scheme, as shown by numerical simulations, is promising on several accounts:

- It is applicable to any point absorber that can be well described by a linear model;
- It can handle constraints on oscillation amplitude and velocity;
- Observability of the system allows for the estimation of the wave-excitation force by soft sensing;
- The sequence of wave-excitation estimates could be extrapolated to obtain a prediction of the wave excitation, which could be used in the MPC algorithm;
- Resistive losses such as those associated with energy conversion can be accounted for by the objective function in order to obtain better performance.

Further improvement of this control scheme for wave-energy point absorbers is the subject of current research.

ACKNOWLEDGMENTS

The first author is a research fellow funded by the Marie Curie Actions WaveTrain 2 training network and is a member of the International Network on Offshore Renewable Energy (INORE).

REFERENCES

Babarit A. & Clément A.H. 2006. Optimal latching control of a wave energy device in regular and irregular waves. *Applied Ocean Research*, 28(2), 77-91.

Bacelli G., Gilloteaux J.C. & Ringwood J. 2009. A predictive controller for a heaving buoy producing potable water. In *Proc. of the European Control Conference 2009*. August 23-26. Budapest, Hungary.

Bertsekas D.P. 2005. *Dynamic programming and optimal control, vol. 1*. Athena Scientific, 3rd edition.

Boyd S. & Vandenberghe L. 2004. *Convex optimization*. Cambridge University Press.

Budal K. & Falnes J. 1977. Optimum operation of improved wave-power converter. *Marine Science Communications*, 3(2), 133-150.

Budal K. *et al*. 1982. The Norwegian wave-power buoy project. In *Proc. of the Second Symposium on Wave & Tidal Energy Utilization*, 323-344, Trondheim, Norway.

Cretel J., Lewis A.W., Lightbody G. & Thomas G.P. 2010. An application of model predictive control to a wave energy point absorber. In *Proc. of the IFAC conference on Control Methodologies and Technology for Energy Efficiency*, March 29-31, Vilamoura, Portugal.

Cummins W.E. 1962. The impulse response function and ship motions. *Schiffstechnik*, 9, 101-109.

Duclos G., Clément A.H. & Chatry G. 2001. Absorption of outgoing waves in a numerical wave tank using a self-adaptive boundary condition. *International Journal of Offshore and Polar Engineering*, 11(2), 104-111.

Eidsmoen H. 1998. Tight-moored amplitude-limited heaving buoy wave energy converter with phase control. *Applied Ocean Research*, 20(3), 157-161.

Falcão A.F. de O. 2007. Phase control through load control of oscillating-body wave energy converters with hydraulic PTO system. In *Proc. 7th European Wave and Tidal Energy Conference*, Porto, Portugal.

Falnes J. 1980. Radiation impedance matrix and optimum power absorption for interacting oscillators in surface waves. *Applied Ocean Research*, 2(2), 75-80.

Falnes J. 2002a. *Ocean waves and oscillating systems: linear interaction including wave-energy extraction*. Cambridge University Press.

Falnes J. 2002b. Optimum control of oscillation of wave-energy converters. *International Journal of Offshore and Polar Engineering*, 12(2), 147-155.

Falnes J. & Budal K. 1978. Wave-power absorption by point absorbers. *Norwegian Maritime Research*, 6(4), 2-11.

Franklin G.F., Powell J.D. & Workman M.L. 1990. *Digital control of dynamic systems*. Addison-Wesley, 2nd edition. Ch. 4.

Fusco, F. & Ringwood, J.V. 2010. Short-term wave forecasting for real-time control of wave energy converters. *IEEE Transactions on Sustainable Energy*, 1(2), 99-106.

Gieske P. 2007. *Model predictive control of a wave energy converter: Archimedes Wave Swing*. M.Sc. thesis, Delft University of Technology, the Netherlands.

Hals J., Falnes J. and Moan, T. 2011. Constrained optimal control of a heaving buoy wave-energy converter. *Journal of Offshore Mechanics and Arctic Engineering*, ASME, 133, 011401.

Hayes M.H. 1996. *Statistical digital signal processing and modelling*. Wiley. Ch. 4.

Hoskin R.E. 1988. *Optimal control techniques for water power generation*. Ph.D. thesis, University of Reading, UK.

Maciejowski J.M. 2002. *Predictive control with constraints*. Prentice Hall.

Molinas M. *et al*. 2007. Power electronics as grid interface for actively controlled wave energy converters. *International Conference on Clean Electrical Power*, Capri, Italy.

Naito S. & Nakamura S. 1985. Wave energy absorption in irregular waves by feed-forward control system. In *Hydrodynamics of ocean wave-energy utilization*, ed. by D.V.Evans & A.F. de O. Falcão, 269-280. IUTAM Symposium, Lisbon. Springer-Verlag, Berlin.

Newman J.N. 1977. *Marine Hydrodynamics*. MIT Press.

Payne G.S. *et al.* 2005. Potential of digital displacement™ hydraulics for wave energy conversion. In *Proc. of the 6th European Wave and Tidal Energy Conference*, August 29 – September 2, Glasgow, UK.

Price A.A.E., Forehand D.I.M. & Wallace A.R. 2009. Time-span of future information necessary for theoretical acausal optimal control of wave energy converters. In *Proc. of the European Control Conference 2009*. August 23-26. Budapest, Hungary.

Rossiter J.A. 2003. *Model-based predictive control: a practical approach*. CRC Press. Ch.3.

Salter S.H., Taylor J.R.M. & Caldwell N.J. 2002. Power conversion mechanisms for wave energy. *Proc. of the Institution of Mechanical Engineers*, *Part M—Journal of Engineering for the Maritime Environment*, 216, 1-27.

Thomas G.P. & Evans D.V. 1981. Arrays of three-dimensional wave-energy absorbers. *Journal of Fluid Mechanics*, 108, 67-88.